Hot and dense hadronic matter in an effective mean field approach

A. Lavagno

Dipartimento di Fisica, Politecnico di Torino and INFN, Sezione di Torino, Italy

We investigate the equation of state of hadronic matter at finite values of baryon density and temperature reachable in high energy heavy ion collisions. The analysis is performed by requiring the Gibbs conditions on the global conservation of baryon number, electric charge fraction and zero net strangeness. We consider an effective relativistic mean-field model with the inclusion of Δ-isobars, hyperons and lightest pseudoscalar and vector mesons degrees of freedom. In this context, we study the influence of the Δ-isobars degrees of freedom in the hadronic equation of state and, in connection, the behavior of different particle-antiparticle ratios and strangeness production.

I. INTRODUCTION

The determination of the properties of nuclear matter as function of density and temperature is a fundamental task in nuclear and subnuclear physics. Heavy ion collisions experiments open the possibility to investigate strongly interacting compressed nuclear matter exploring in laboratory the structure of the QCD phase diagram [1–4]. The extraction of information about the Equation of State (EOS) at different densities and temperatures by means of intermediate and high energy heavy ion collisions is a very difficult task and can be realized only indirectly by comparing the experimental data with different theoretical models, such as, for example, fluid-dynamical models. The EOS at density below the saturation density of nuclear matter ($\rho_0 \approx 0.16$ fm^{-3}) is relatively well known due to the large amount of experimental nuclear data available. At larger density there are many uncertainties; the strong repulsion at short distances of nuclear force makes, in fact, the compression of nuclear matter quite difficult. However, in relativistic heavy ion collisions the baryon density can reach values of a few times the saturation nuclear density and/or high temperatures. The future CBM (Compressed Baryonic Matter) experiment of FAIR (Facility of Antiproton and Ion Research) project at GSI Darmstadt, will make it possible to create compressed baryonic matter with a high net baryon density [5–7]. In this direction interesting results have been obtained at low SPS energy and are foreseen at a low-energy scan at RHIC [8–12].

On the other hand, the information coming from experiments with heavy ions at intermediate and high energy collisions is that the EOS depends on the energy beam but also on the electric charge fraction Z/A of the colliding nuclei, especially at not too high temperature [13, 14]. Moreover, the analysis of observations of neutron stars, which are composed of β-stable matter for which $Z/A \leq 0.1$, can also provide hints on the structure of extremely asymmetric matter at high density [15, 16].

To well understand the structure of the phase diagram and the supposed deconfinement quark-gluon phase transition at large density and finite temperature, it is crucial to know accurately the EOS of the hadronic as well as the quark-gluon phase. Concerning the hadronic phase, hadron resonance gas models turned out to be very successful in describing particle abundances produced in (ultra)relativistic heavy ion collisions [17–19]. In this framework, to take phenomenologically into account the interaction between hadrons at finite densities, finite size corrections have been considered in the excluded volume approximation [20–25].

From a more microscopic point of view, the hadronic EOS should reproduce properties of equilibrium nuclear matter such as, for example, saturation density, binding energy, symmetric energy coefficient, compression modulus. Some other constraints on the behavior of the EOS come out from analysis of the experimental flow data of heavy ion collisions at intermediate energy [26] and, moreover, there are different indirect contraints/indications related to astrophysical bounds on high density β-equilibrium compact stars [15, 27]. In connection with these matters, Walecka type Relativistic Mean-Field (RMF) models have been widely successfully used for describing the properties of finite nuclei as well as dense and finite temperature nuclear matter [28–32]. It is relevant to point out that such RMF models usually do not respect chiral symmetry. Furthermore, the repulsive vector field is proportional to the net baryon density, therefore, standard RMF models do not appear, in principle, fully appropriate for very low density and high temperature regime. In this context, let us observe that has been recently proposed a phenomenological RMF model in order to calculate the EOS of hadronic matter in a broad density-temperature region by considering masses and coupling constants depending on the σ-meson field [33]. In that approach, motivated by the Brown-Rho scaling hypothesis, a not chiral symmetric model simulates a chiral symmetric restoration with a temperature increase. On the other hand, sophisticated relativistic chiral SU(3) models are also developed to take into account particle ratios at RHIC and baryon resonances impact on the chiral phase transition [34, 35].

In regime of finite values of density and temperature, a state of high density resonance matter may be formed and the $\Delta(1232)$-isobars degrees of freedom are expected to play a central role [36]. Transport model calculations

and experimental results indicate that an excited state of baryonic matter is dominated by the Δ-resonance at the energy from AGS to RHIC [37–42]. Moreover, in the framework of the non-linear Walecka model, it has been predicted that a phase transition from nucleonic matter to Δ-exited nuclear matter can take place and the occurrence of this transition sensibly depends on the Δ-mesons coupling constants [43, 44]. Referring to QCD finite-density sum rules results, which predict that there is a larger net attraction for a Δ-isobar than for a nucleon in the nuclear medium [45], the range of values for the Δ-mesons coupling constants has been confined within a triangle relation [46]. Whether stable Δ-exited nuclear matter exists or not is still a controversial issue because little is actually known about the Δ coupling constants with the scalar and vector mesons. In any case, it has been pointed out that the existence of degrees of freedom related to Δ-isobars can be very relevant in relativistic heavy ion collisions and in the core of neutron stars [44, 47, 48]. Although several papers have investigated the influence of Δ-isobars in the nuclear EOS, we believe that, especially in presence of asymmetric and strange hadronic matter, a systematic investigation at finite densities and temperatures has been lacking.

In this paper we are going to study the hadronic EOS by means of an effective RMF model with the inclusion of the full octet of baryons, the Δ-isobars degrees of freedom and the lightest pseudoscalar and vector mesons. These last particles are considered in the so-called one-body contribution, taking into account their effective chemical potentials depending on the self-consistent interaction between baryons. The main goal is to investigate how the constraints on the global conservation of the baryon number, electric charge fraction and strangeness neutrality, in the presence of Δ-isobars degrees of freedom, hyperons and strange mesons, influence the behavior of the EOS in regime of finite values of baryon density and temperature. Moreover, we plan to show the relevance of Δ-isobars for different coupling constants and how its presence influences several particle ratios and strangeness production for three different parameters sets, compatible with experimental constraints.

The paper is organized as follows. In Section II, we present the model with a detailed discussion on the hyperons-mesons couplings and on the chemical equilibrium conditions. In order to better clarify the role of Δ-isobars and strange particles in symmetric and asymmetric nuclear matter, our results are presented in Section III which is divided in three subsections: in A) we study the equation of state of nucleons and Δ-isobars in symmetric nuclear matter at zero and finite temperature; in B) we extend the investigation by including hyperons, non-strange and strange mesons in asymmetric nuclear matter and by requiring the zero net strangeness condition. Strangeness production and different particle-antiparticle ratios are considered in subsection C). Finally, we summarize our main conclusions in Section IV.

II. HADRONIC EQUATION OF STATE

The basic idea of the RMF model, first introduced by Walecka and Boguta-Bodmer in the mid-1970s [49, 50], is the interaction between baryons through the exchange of mesons. In the original version we have an isoscalar-scalar σ meson field which produces the medium range attraction and the exchange of isoscalar-vector ω mesons responsible for the short range repulsion. The saturation density and binding energy per nucleon of nuclear matter can be fitted exactly in the simplest version of this model but other properties of nuclear matter, as e.g. incompressibility, cannot be well reproduced. To overcome these difficulties, the model has been modified introducing in the Lagrangian two terms of self-interaction for the σ mesons which are crucial to reproduce the empirical incompressibility of nuclear matter and the effective mass of nucleons M_N^*. Moreover, the introduction of an isovector-vector ρ meson allows to reproduce the correct value of the empirical symmetry energy [51] and an isovector-scalar field, a virtual $a_0(980)$ δ-meson, has been been studied for asymmetric nuclear matter and for heavy ion collisions [13, 52].

The total Lagrangian density $\mathcal{L}$ can be written as

$$\mathcal{L} = \mathcal{L}_{\rm om} + \mathcal{L}_{\Delta} + \mathcal{L}_{\rm qfm}\,, \tag{1}$$

where $\mathcal{L}_{\rm om}$ stands for the full octet of lightest baryons $(p,\ n,\ \Lambda,\ \Sigma^+,\ \Sigma^0,\ \Sigma^-,\ \Xi^0,\ \Xi^-)$ interacting with σ, ω, ρ, δ mesons fields; $\mathcal{L}_{\Delta}$ corresponds to the degrees of freedom for the Δ-isobars $(\Delta^{++},\ \Delta^+,\ \Delta^0,\ \Delta^-)$ and $\mathcal{L}_{\rm qfm}$ is related to a (quasi)free gas of the lightest pseudoscalar and vector mesons with an effective chemical potential (see below for details). In the regime of density and temperature we are mostly interested, we expect that the inclusion of the other decuplet baryons will produce only a small change in the overall results.

The RMF model for the self-interacting full octet of baryons $(J^P = 1/2^+)$ was originally studied by Glendenning [53] with the following standard Lagrangian

$$\mathcal{L}_{\text{om}} = \sum_k \overline{\psi}_k \left[i\,\gamma_\mu\,\partial^\mu - (M_k - g_{\sigma k}\,\sigma - g_{\delta k}\,\vec{t}\cdot\vec{\delta}) - g_{\omega k}\,\gamma_\mu\,\omega^\mu - g_{\rho k}\,\gamma_\mu\,\vec{t}\cdot\vec{\rho}^{\,\mu} \right] \psi_k + \frac{1}{2}(\partial_\mu\sigma\partial^\mu\sigma - m_\sigma^2\sigma^2) - U(\sigma)$$

$$+ \frac{1}{2}\,m_\omega^2\,\omega_\mu\omega^\mu + \frac{1}{4}\,c\,(g_{\omega N}^2\,\omega_\mu\omega^\mu)^2 + \frac{1}{2}\,m_\rho^2\,\vec{\rho}_\mu\cdot\vec{\rho}^{\,\mu} + \frac{1}{2}(\partial_\mu\vec{\delta}\,\partial^\mu\vec{\delta} - m_\delta^2\,\vec{\delta}^2) - \frac{1}{4}F_{\mu\nu}F^{\mu\nu} - \frac{1}{4}\vec{G}_{\mu\nu}\vec{G}^{\mu\nu}, \qquad (2)$$

where the sum runs over all baryons octet, M_k is the vacuum baryon mass of index k, the quantity $\vec{t}$ denotes the isospin operator which acts on the baryon and the field strength tensors for the vector mesons are given by the usual expressions $F_{\mu\nu} \equiv \partial_\mu\omega_\nu - \partial_\nu\omega_\mu$, $\vec{G}_{\mu\nu} \equiv \partial_\mu\vec{\rho}_\nu - \partial_\nu\vec{\rho}_\mu$. The $U(\sigma)$ is a nonlinear self-interaction potential of σ meson

$$U(\sigma) = \frac{1}{3}a\,(g_{\sigma N}\,\sigma)^3 + \frac{1}{4}\,b\,(g_{\sigma N}\,\sigma^4), \qquad (3)$$

introduced by Boguta and Bodmer [50] to achieve a reasonable compressibility for equilibrium normal nuclear matter. We have also taken into account the additional self-interaction ω meson field: $c\,(g_{\omega N}^2\,\omega_\mu\omega^\mu)^2/4$ suggested by Bodmer [54] to get a good agreement with Dirac-Brückner calculations at high density and to achieve a more satisfactory description of the properties of finite nuclei in the mean field approximation.

By taking into account only the on-shell Δs, the Lagrangian density concerning the Δ-isobars can be expressed as [44]

$$\mathcal{L}_\Delta = \overline{\psi}_{\Delta\,\nu}\left[i\gamma_\mu\partial^\mu - (M_\Delta - g_{\sigma\Delta}\sigma) - g_{\omega\Delta}\gamma_\mu\omega^\mu\right]\psi_\Delta^\nu, \quad (4)$$

where ψ_Δ^ν is the Rarita-Schwinger spinor for the Δ baryon. Due to the uncertainty on the Δ-meson coupling constants, we limit ourselves to consider only the coupling with the σ and ω mesons fields, more explored in the literature [43–46].

In the RMF approach, baryons are considered as Dirac quasiparticles moving in classical mesons fields and the field operators are replaced by their expectation values. In this context, it is relevant to remember that the RMF model does not respect chiral symmetry and the contribution coming from the Dirac-sea and quantum fluctuation of the meson fields are neglected. As a consequence, the field equations in RMF approximation have the fol-

lowing form

$$\left(i\gamma_\mu\partial^\mu - M_k^* - g_{\omega k}\gamma^0\omega - g_{\rho k}\gamma^0 t_{3k}\rho\right)\psi_k = 0, \quad (5)$$

$$\left(i\gamma_\mu\partial^\mu - M_\Delta^* - g_{\omega\Delta}\gamma^0\omega\right)\psi_\Delta = 0, \qquad (6)$$

$$m_\sigma^2\sigma + a\,g_{\sigma N}^3\,\sigma^2 + b\,g_{\sigma N}^4\,\sigma^3 = \sum_i g_{\sigma i}\,\rho_i^S, \qquad (7)$$

$$m_\omega^2\omega + c\,g_{\omega N}^4\,\omega^3 = \sum_i g_{\omega i}\,\rho_i^B, \qquad (8)$$

$$m_\rho^2\rho = \sum_i g_{\rho i}\,t_{3i}\,\rho_i^B, \qquad (9)$$

$$m_\delta^2\delta = \sum_i g_{\delta i}\,t_{3i}\,\rho_i^S, \qquad (10)$$

where $\sigma = \langle\sigma\rangle$, $\omega = \langle\omega^0\rangle$, $\rho = \langle\rho_3^0\rangle$ and $\delta = \langle\delta_3\rangle$ are the nonvanishing expectation values of mesons fields. The effective mass of k-th baryon octet, comparing in Eq.(5), is given by

$$M_k^* = M_k - g_{\sigma k}\sigma - g_{\delta k}t_{3k}\delta, \qquad (11)$$

and the effective mass of Δ-isobar, comparing in Eq.(6), is given by

$$M_\Delta^* = M_\Delta - g_{\sigma\Delta}\sigma. \qquad (12)$$

In the mesons fields equations, Eqs.(7)-(10), the sums run over all considered baryons (octet and Δs) and ρ_i^B and ρ_i^S are the baryon density and the baryon scalar density of the particle of index i, respectively. They are given by

$$\rho_i^B = \gamma_i \int \frac{\mathrm{d}^3k}{(2\pi)^3}\,[f_i(k) - \overline{f}_i(k)], \qquad (13)$$

$$\rho_i^S = \gamma_i \int \frac{\mathrm{d}^3k}{(2\pi)^3}\,\frac{M_i^*}{E_i^*}\,[f_i(k) + \overline{f}_i(k)], \qquad (14)$$

where $\gamma_i = 2J_i+1$ is the degeneracy spin factor of the i-th baryon ($\gamma_{\text{octet}} = 2$ for the baryon octet and $\gamma_\Delta = 4$) and $f_i(k)$ and $\overline{f}_i(k)$ are the fermion particle and antiparticle distributions

$$f_i(k) = \frac{1}{\exp\{(E_i^*(k) - \mu_i^*)/T\} + 1}, \qquad (15)$$

$$\overline{f}_i(k) = \frac{1}{\exp\{(E_i^*(k) + \mu_i^*)/T\} + 1}. \qquad (16)$$

The baryon effective energy is defined as $E_i^*(k) = \sqrt{k^2 + M_i^{*2}}$. The chemical potentials μ_i are given in

terms of the effective chemical potentials μ_i^* by means of the following relation

$$\mu_i = \mu_i^* + g_{\omega i}\,\omega + g_{\rho i}\,t_{3i}\,\rho\,, \qquad (17)$$

where t_{3i} is the third component of the isospin of i-th baryon.

Because we are going to describe the nuclear EOS at finite density and temperature with respect to strong interaction, we have to require the conservation of three "charges": baryon number (B), electric charge (C) and strangeness number (S). Each conserved charge has a conjugated chemical potential and the systems is described by three independent chemical potentials: μ_B, μ_C and μ_S. Therefore, the chemical potential of particle of index i can be written as

$$\mu_i = b_i\,\mu_B + c_i\,\mu_C + s_i\,\mu_S\,, \qquad (18)$$

where b_i, c_i and s_i are, respectively, the baryon, the electric charge and the strangeness quantum numbers of i-th hadronic species.

The thermodynamical quantities can be obtained from the grand potential Ω_B in the standard way. More explicitly, the baryon pressure $P_B = -\Omega_B/V$ and the energy density ϵ_B can be written as

$$
\begin{aligned}
P_B \;=\; & \frac{1}{3}\sum_i \gamma_i \int \frac{\mathrm{d}^3 k}{(2\pi)^3}\,\frac{k^2}{E_i^*(k)}\,[f_i(k)+\overline{f}_i(k)] \\
& -\frac{1}{2}\,m_\sigma^2\,\sigma^2 - U(\sigma) + \frac{1}{2}\,m_\omega^2\,\omega^2 + \frac{1}{4}\,c\,(g_{\omega N}\,\omega)^4 \\
& + \frac{1}{2}\,m_\rho^2\,\rho^2 - \frac{1}{2}\,m_\delta^2\,\delta^2,
\end{aligned}
\qquad (19)
$$

$$
\begin{aligned}
\epsilon_B \;=\; & \sum_i \gamma_i \int \frac{\mathrm{d}^3 k}{(2\pi)^3}\,E_i^*(k)\,[f_i(k)+\overline{f}_i(k)] \\
& + \frac{1}{2}\,m_\sigma^2\,\sigma^2 + U(\sigma) + \frac{1}{2}\,m_\omega^2\,\omega^2 + \frac{3}{4}\,c\,(g_{\omega N}\,\omega)^4 \\
& + \frac{1}{2}\,m_\rho^2\,\rho^2 + \frac{1}{2}\,m_\delta^2\,\delta^2\,.
\end{aligned}
\qquad (20)
$$

The numerical evaluation of the above thermodynamical quantities can be performed if the meson-nucleon, meson-Δ and meson-hyperon coupling constants are known. Concerning the meson-nucleon coupling constants ($g_{\sigma N}$, $g_{\omega N}$, $g_{\rho N}$, $g_{\delta N}$), they are determined to reproduce properties of equilibrium nuclear matter such as the saturation densities, the binding energy, the symmetric energy coefficient, the compression modulus and the effective Dirac mass at saturation. Due to a valuable range of uncertainty in the empirical values that must be fitted, especially for the compression modulus and for the effective Dirac mass, in literature there are different sets of coupling constants. In Table I, we report the parameters sets used in this work. The set marked GM3 is from Glendenning and Moszkowski [55], that labelled NL$\rho\delta$ is from Ref.[52, 56] and TM1 from Ref.[57]. As we will see in next Section, we have limited our investigation to these three parameters sets that are compatible with intermediate heavy ion collisions constraints and extensively used

in various high density astrophysical applications. Let us remark that the first two parameters sets have the same saturated compressibility K and an almost equal value of the nucleon effective mass M_N^*, significantly larger than the TM1 one. Therefore, the GM3 and NL$\rho\delta$ models will fail to reproduce the correct spin-orbit splittings in finite nuclei [58]. On the other hand, the TM1 parameters set have a larger value of K but a sensibly lower value of M_N^*. As we will see, these different saturation properties of nuclear matter are strongly correlated to the formation of Δ-isobar matter at finite density and temperature.

The implementation of hyperons degrees of freedom comes from determination of the corresponding meson-hyperon coupling constants that have been fitted to hypernuclear properties. Following Ref.s[59–63], we can use the SU(6) simple quark model and obtain the relations

$$
\begin{aligned}
& \frac{1}{3}g_{\omega N} = \frac{1}{2}g_{\omega\Lambda} = \frac{1}{2}g_{\omega\Sigma} = g_{\omega\Xi}\,, \\
& g_{\rho N} = \frac{1}{2}g_{\rho\Sigma} = g_{\rho\Xi}\,, \quad g_{\rho\Lambda} = 0\,, \\
& g_{\delta N} = \frac{1}{2}g_{\delta\Sigma} = g_{\delta\Xi}\,, \quad g_{\delta\Lambda} = 0\,.
\end{aligned}
\qquad (21)
$$

In addition, we can fix the scalar σ meson-hyperon ($g_{\sigma Y}$) coupling constants to the potential depth of the corresponding hyperon in normal dense matter taking into account the following recent results [63–66]

$$U_\Lambda^N = -28\,\mathrm{MeV}, \quad U_\Sigma^N = +30\,\mathrm{MeV}, \quad U_\Xi^N = -18\,\mathrm{MeV}\,. \qquad (22)$$

In Table II, we report the obtained ratios $x_{\sigma Y} = g_{\sigma Y}/g_{\sigma N}$ and the vacuum hyperon masses are listened in Table III. In this context, let us mention that the two additional mesons fields $f_0(975)$ and $\phi(1020)$, usually introduced to simulate the hyperon-hyperon attraction observed in $\Lambda - \Lambda$ hypernuclei [62, 63], do not play a significant role in the considered range of density and temperature and, therefore, we have neglected their contributions.

As discussed in the Introduction, the aim of this work is to describe the EOS at finite values of density and temperature. Especially at low baryon density and high temperature, the contribution of the lightest pseudoscalar and vector mesons to the total thermodynamical potential (and, consequently, to the other thermodynamical quantities) becomes very important. On the other hand, the contribution of the π mesons (and other pseudoscalar and pseudovector fields) vanishes at the mean field level. From a phenomenological point of view, we can take into account the meson particles degrees of freedom by adding their one-body contribution to the thermodynamical potential, i.e. the contribution of an ideal Bose gas with an effective chemical potential μ_j^*, depending self-consistently from the mesons fields. Following this scheme, we can evaluate the pressure P_M, the energy density ϵ_M and the particle density ρ_j^M of mesons

TABLE I: Nuclear matter properties and nucleon coupling constants of the parameters sets used in the calculation. The energy per particle is E/A=16.3 MeV, calculated at the saturation density ρ_0 with a compression modulus K and effective mass M_N^* (the nucleon mass M_N is fixed to 939 MeV for GM3 and NL$\rho\delta$, M_N = 938 MeV in TM1 parameters set). The symmetry energy is denoted by a_{sym}. In the parameters set NL$\rho\delta$ the additional coupling to δ meson is fixed to $g_{\delta N}/m_\delta$ =3.162 fm.

	ρ_0	K	M_N^*/M_N	a_{sym}	$\frac{g_{\sigma N}}{m_\sigma}$	$\frac{g_{\omega N}}{m_\omega}$	$\frac{g_{\rho N}}{m_\rho}$	a	b	c
	(fm^{-3})	(MeV)		(MeV)	(fm)	(fm)	(fm)	(fm^{-1})		
GM3	0.153	240	0.78	32.5	3.151	2.195	2.189	0.04121	-0.00242	-
NL$\rho\delta$	0.160	240	0.75	30.5	3.214	2.328	3.550	0.0330	-0.0048	-
TM1	0.145	281	0.63	36.9	3.871	3.178	2.374	0.00717	0.00006	0.00282

TABLE II: Ratios of the scalar σ-meson coupling constants for hyperons: $x_{\sigma Y} = g_{\sigma Y}/g_{\sigma N}$.

	$x_{\sigma\Lambda}$	$x_{\sigma\Sigma}$	$x_{\sigma\Xi}$
GM3	0.606	0.328	0.322
NL$\rho\delta$	0.606	0.361	0.320
TM1	0.616	0.447	0.319

as

$$P_M = \frac{1}{3}\sum_j \gamma_j \int \frac{\mathrm{d}^3 k}{(2\pi)^3}\, \frac{k^2}{E_j(k)}\, g_j(k)\,, \qquad (23)$$

$$\epsilon_M = \sum_j \gamma_j \int \frac{\mathrm{d}^3 k}{(2\pi)^3}\, E_j(k)\, g_j(k)\,, \qquad (24)$$

$$\rho_j^M = \gamma_j \int \frac{\mathrm{d}^3 k}{(2\pi)^3}\, g_j(k)\,, \qquad (25)$$

where $\gamma_j = 2J_j + 1$ is the degeneracy spin factor of the j-th meson ($\gamma = 1$ for pseudoscalar mesons and $\gamma = 3$ for vector mesons), the sum runs over the lightest pseudoscalar mesons (π, K, $\overline{K}$, η, η') and the lightest vector mesons (ρ, ω, K^*, $\overline{K}^*$, ϕ), considering the contribution of particle and antiparticle separately. In Eq.s(23)-(25) the function $g_j(k)$ is the boson particle distribution (the corresponding antiparticle distribution $\overline{g}_j(k)$ will be obtained with the substitution $\mu_j^* \to -\mu_j^*$) given by

$$g_j(k) = \frac{1}{\exp\{(E_j(k) - \mu_j^*)/T\} - 1}\,, \qquad (26)$$

where $E_j(k) = \sqrt{k^2 + m_j^2}$ and m_j is the j-th meson mass (see Table III). Moreover, the boson integrals are subjected to the constraint $|\mu_j^*| \le m_j$, otherwise Bose condensation becomes possible (as we will see in the next Section, this condition is never achieved in the range of density and temperature investigated in this paper). The values of the effective meson chemical potentials μ_j^* are obtained from the "bare" ones μ_j, given in Eq.(18), and subsequently expressed in terms of the corresponding effective baryon chemical potentials, respecting the strong interaction [72]. For example, we have from Eq.(18) that $\mu_{\pi^+} = \mu_{\rho^+} = \mu_C \equiv \mu_p - \mu_n$ and the corresponding effec-

tive chemical potential can be written as

$$\begin{aligned} \mu_{\pi^+(\rho^+)}^* &\equiv \mu_p^* - \mu_n^* \\ &= \mu_p - \mu_n - g_{\rho N}\rho\,, \end{aligned} \qquad (27)$$

where the last equivalence follows from Eq.(17).

Analogously, by setting $x_{\omega\Lambda} = g_{\omega\Lambda}/g_{\omega N}$, we have

$$\begin{aligned} \mu_{K^+(K^{*+})}^* &\equiv \mu_p^* - \mu_{\Lambda(\Sigma^0)}^* \\ &= \mu_p - \mu_\Lambda - (1 - x_{\omega\Lambda})g_{\omega N}\omega - \frac{1}{2}g_{\rho N}\rho\,, \end{aligned} \qquad (28)$$

$$\begin{aligned} \mu_{K^0(K^{*0})}^* &\equiv \mu_n^* - \mu_{\Lambda(\Sigma^0)}^* \\ &= \mu_n - \mu_\Lambda - (1 - x_{\omega\Lambda})g_{\omega N}\omega + \frac{1}{2}g_{\rho N}\rho\,, \end{aligned} \qquad (29)$$

while the others strangeless neutral mesons have a vanishing chemical potential. Thus, the effective meson chemical potentials are coupled with the meson fields related to the interaction between baryons. As we will see in the next Section, this assumption represents a crucial feature in the EOS at finite density and temperature and can be seen somehow in analogy with the hadron resonance gas within the excluded-volume approximation. There the hadronic system is still regarded as an ideal gas but in the volume reduced by the volume occupied by constituents (usually assumed as a phenomenological model parameter), here we have a (quasi free) mesons gas but with an effective chemical potential which contains the self-consistent interaction of the mesons fields.

Finally, the total pressure and energy density will be

$$P = P_B + P_M\,, \qquad (30)$$

$$\epsilon = \epsilon_B + \epsilon_M\,. \qquad (31)$$

At a given temperature T, all the above equations must be evaluated self-consistently by requiring the baryon, electric charge fraction and strangeness numbers conservation [68]. Therefore, at a given baryon density ρ_B, a given Z/A net electric charge fraction ($\rho_C = Z/A\,\rho_B$) and a zero net strangeness of the system ($\rho_S = 0$), the chemical potentials μ_B, μ_C and μ_S are univocally deter-

TABLE III: Vacuum masses (given in MeV) of the considered hadronic particles.

M_N	M_Λ	M_Σ	M_Δ	M_Ξ	M_π	M_K	M_η	$M_{\eta'}$	M_{K^*}	M_ρ	M_ω	M_ϕ
939	1116	1189	1232	1315	140	494	547	958	892	771	782	1020

mined by the following equations

$$\rho_B = \sum_i b_i\, \rho_i(T, \mu_B, \mu_C, \mu_S)\,, \qquad (32)$$

$$\rho_C = \sum_i c_i\, \rho_i(T, \mu_B, \mu_C, \mu_S)\,, \qquad (33)$$

$$\rho_S = \sum_i s_i\, \rho_i(T, \mu_B, \mu_C, \mu_S)\,, \qquad (34)$$

where the sums run over all considered particles.

III. RESULTS AND DISCUSSION

A. Equation of state of pnΔ symmetric nuclear matter

Let us start our numerical investigation by considering the symmetric hadronic EOS using the model discussed here. In order to better focalize the role of Δ-isobar degrees of freedom, we will limit this first subsection to consider only protons, neutrons and Δ particles.

In Fig. 1, we report the pressure as a function of the baryon density (in units of the nuclear saturation density ρ_0) in the limit of zero temperature. Among the several parameters sets, we choose the three sets: GM3, NL$\rho\delta$, TM1 (see Table 1 for details) that meet in a satisfactory way the region, reported as shaded area, of pressures consistent with the experimental flow data of heavy ion collisions at intermediate energy, analyzed by using the Boltzmann equation model [26]. Furthermore, these parameters sets are largely used to describe the hadronic EOS on high density β-equilibrium compact stars [13, 27, 32].

At the scope of giving a roughly indication of the presence of the Δ-isobars degrees of freedom from the point of view of the stiffness of the EOS, in Fig. 1, we show the behavior of the pressure corresponding only to nucleons (monotonic curves) and nucleons and Δ (non-monotonic curves) with the scalar $r_s = g_{\sigma\Delta}/g_{\sigma N}$ and vector $r_v = g_{\omega\Delta}/g_{\omega N}$ meson-Δ couplings ratios. Let us note in this context that, when a metastable condition for Δ-isobars is not realized (see discussion below), decays rates are not taken into account. Moreover, a further softening of the EOS can occur considering the degrees of freedom of the other hadronic particles. At zero temperature and symmetric nuclear matter these effects occur at very high density and, as anticipated, we will consider them separately in the next subsections.

To better understand the dependence of the EOS on the meson-Δ coupling constants for the different parameters sets, we start by reporting in Fig. 2 the energy per
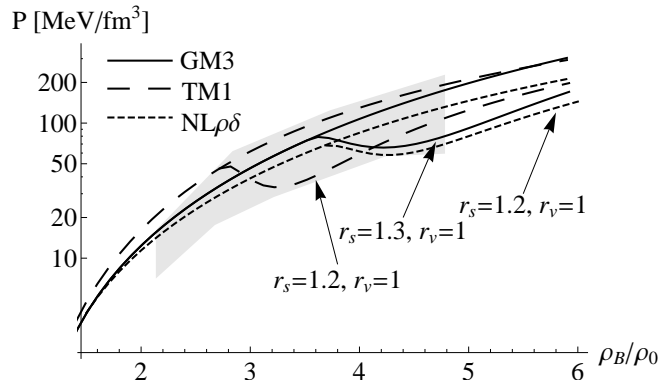

FIG. 1: Pressure as a function of the baryon density (in units of the nuclear saturation density ρ_0) for the symmetric nuclear matter at zero temperature for three different EOSs and Δ coupling ratios (absence of Δ contribution in the monotonic curves). The shaded region corresponds to the limits obtained from the analysis of Ref.[26].

baryon versus baryon density at zero temperature and GM3 parameters set. The curves (labelled with a, b, c, d, e, f) represent different values of the scalar r_s and vector r_v meson-Δ couplings ratios. In setting these coupling constants we have required, as in Ref.[46], that i) the second minimum of the energy per baryon lies above the saturation energy of normal nuclear matter, i.e., in the mixed Δ-nucleon phase only a metastable state can occur; ii) there are no Δ-isobars present at the saturation density; iii) the scalar field is more (equal) attractive and the vector potential is less (equal) repulsive for Δs than for nucleons, in according with QCD finite density calculations [45]. Of course, the choice of couplings that satisfies the above conditions is not unique but exists a finite range of possible values (represented as a triangle region in the plane r_s-r_v) which depends on the particular EOS under consideration [46]. Without loss of generality, we can limit our investigation to move only in a side of such a triangle region by fixing $r_v = 1$ and varying r_s from unity to a maximum value compatible with the conditions mentioned above. Similar conclusions are obtained with any other compatible choice of the two coupling ratios.

In Fig. 3, we compare the energy per baryon for different parameters sets but at a fixed value of the scalar and vector Δ coupling constants. At variance of the parameters sets we have a very different behavior, on the other hand, we obtain comparable features for the three considered parameters sets by means of a rescaling of the Δ couplings. To better clarify this aspect, in Table
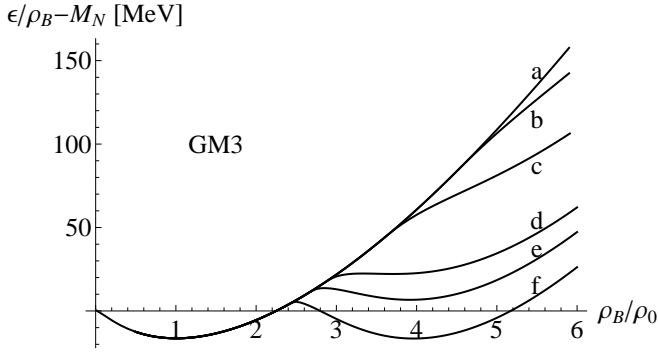
FIG. 2: The energy per baryon versus baryon density at zero temperature and GM3 parameters set with: a) without Δ, b) non-interacting Δ ($r_s = r_v = 0$), c):($r_s = 1.3$, $r_v = 1$), d):($r_s = 1.41$, $r_v = 1$), e):($r_s = 1.45$, $r_v = 1$), f:($r_s = 1.5$, $r_v = 1$).
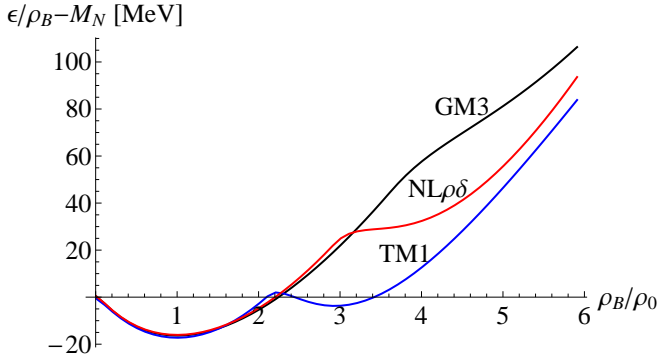

FIG. 3: (Color online) The same as Fig. 2 but for different parameters sets and fixed $r_s = 1.3$ and $r_v = 1$.

IV we report, for the three parameters sets and fixing $r_v = 1$, the values r_s^{II} corresponding to the appearance of the second minimum on the energy per baryon and $r_s^{\max}$ corresponding to the maximum values of r_s compatible with the constraint that the second minimum of the energy per baryon lies above the saturation energy of normal nuclear matter.

In order to get a deeper insight on the dependence of the Δ-isobars from the coupling constants and from the temperature, in Fig. 4, we show the behavior of the effective mass M_Δ^* for different temperatures and Δ

TABLE IV: Values of the r_s^{II} corresponding to the appearance of the second minimum on the energy per baryon and the maximum values $r_s^{\max}$ obtained by requiring that in the mixed Δ-nucleon phase only a metastable state can occur.

	GM3	NL$\rho\delta$	TM1
r_s^{II}	1.41	1.32	1.27
$r_s^{\max}$	1.50	1.41	1.33
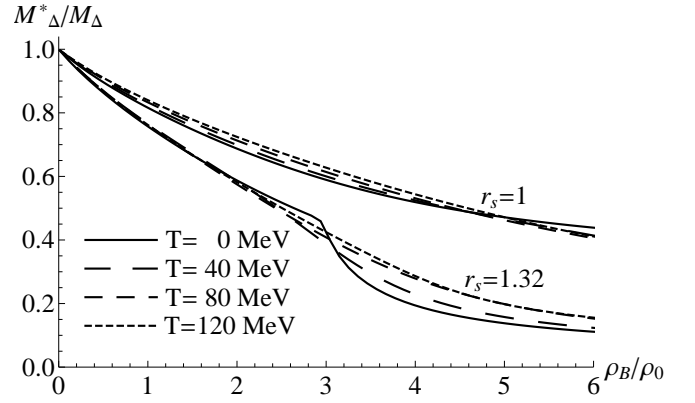
FIG. 4: The Δ effective mass ratios versus the baryon density with $r_s = r_v = 1$ (upper curves) and with $r_s = 1.32$ and $r_v = 1$ (lower curves) for different temperatures. The parameters set used in the calculation is NL$\rho\delta$.

coupling constants ($r_s = r_v = 1$ for upper curves and $r_s = 1.32$ and $r_v = 1$ for lower curves) in the NL$\rho\delta$ parameters sets. Let us note that the coupling ratio of the lower curves corresponds to the appearance of the second minimum of the energy per baryon at zero temperature (metastable state). As we can see, the different behavior of the effective Δ mass from the coupling constants is strongly linked to the different behavior of the energy per baryon versus baryon density and temperature.

In Fig. 5, we show the energy per baryon as a function of the baryon density at $T = 40 \div 100$ MeV for two different Δ scalar coupling ratios r_s and for the TM1 parameters set. As stated before, at zero temperature and fixed $r_v = 1$, there is no second minimum if $r_s = 1$ while it takes place if $r_s = 1.3$ (see Fig. 3 and Table IV). As the temperature increases, the behavior is remarkable different in the case of $r_s = 1.3$ where the first minimum disappears and only the second minimum remains. In the above two figures, the results are reported only for one parameters set, however similar behaviors are obtained with the other sets, if we use comparable meson-Δ coupling ratios. To better clarify this aspect, in Fig. 6, we report the variation of the baryon density, with respect to temperature, corresponding to the position of the second minimum of the energy per baryon for the three different parameters sets. In the comparison, we fix r_s to the average value r_m between r_s^{II} and $r_s^{\max}$ listed in Table IV, for each parameters sets ($r_s = 1.46$ for GM3, $r_s = 1.37$ for NL$\rho\delta$, $r_s = 1.30$ for TM1). For all three sets, the position of the second minimum appears approximately at a constant value of baryon density $\rho_B \approx 3 \div 4\,\rho_0$ until $T \approx 80 \div 100$ MeV. At higher temperatures, as observed in Fig. 5, the first minimum disappears and the second minimum moves rapidly at lower baryon densities. At fixed temperature, the different positions of the second minimum are a direct consequence of the different saturated nucleon effective mass M_N^* in the considered parameters sets. In agreement with the results of Ref.[44],
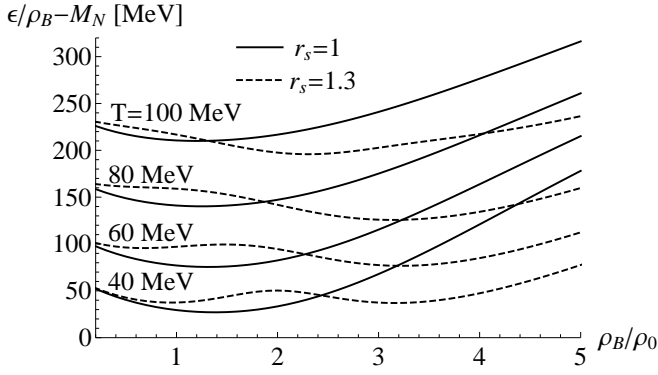
FIG. 5: The energy per baryon versus baryon density for symmetric nuclear matter at different values of temperature and TM1 parameters set. The solid lines correspond to the Δ coupling ratios $r_s = r_v = 1$ and the dashes lines correspond to $r_s = 1.3$ and $r_v = 1$.
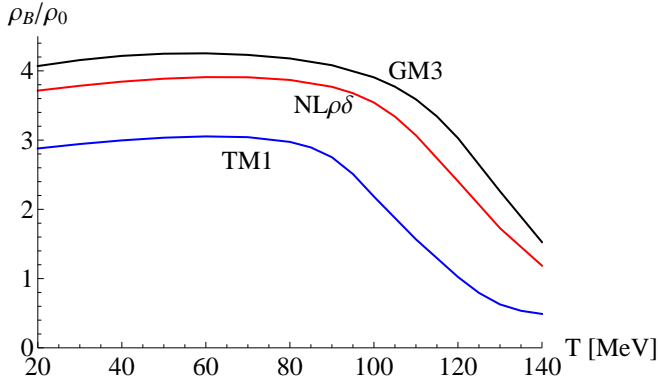

FIG. 6: (Color online) Variation of the baryon density, with respect to temperature, corresponding to the position of the second minimum of the energy per baryon for different parameters sets (see text for details).

FIG. 7: The relative nucleon (solid lines) and Δ (dashed lines) density versus the baryon density with $r_s = r_v = 1$ (upper panel) and with $r_s = 1.32$ and $r_v = 1$ (lower panel) for different values of temperature (in units of MeV). The parameters set used in the calculation is NL$\rho\delta$.

we have, in fact, that a smaller value of M_N^* favors the appearance of a second minimum of the energy per baryon at lower baryon density. Therefore, the position of the second minimum results to be at a sensibly lower baryon density for the TM1 set with respect to the NL$\rho\delta$ and GM3 ones.

In Fig. 7, we report the nucleon (solid lines) and the Δ-isobar (dashed lines) density, normalized to the baryon density, versus the baryon density for different values of temperature (in unit of MeV). We observe that, although the Δ-isobar density seems to be negligible at low temperatures up to very high densities, it becomes relevant by increasing the temperature even for $r_s = r_v = 1$ (upper panel). Moreover, in the case of $r_s = 1.32$ and $r_v = 1$ (lower panel), the Δ particle density becomes comparable to the nucleon density in the range of $T \approx 80 \div 120$ MeV and $\rho_B \approx 1 \div 2.5\,\rho_0$; values that can be reached in high energy heavy ion collisions. This behavior has been obtained for the NL$\rho\delta$ parameters set but is common for all three considered sets even if, at fixed temperature and
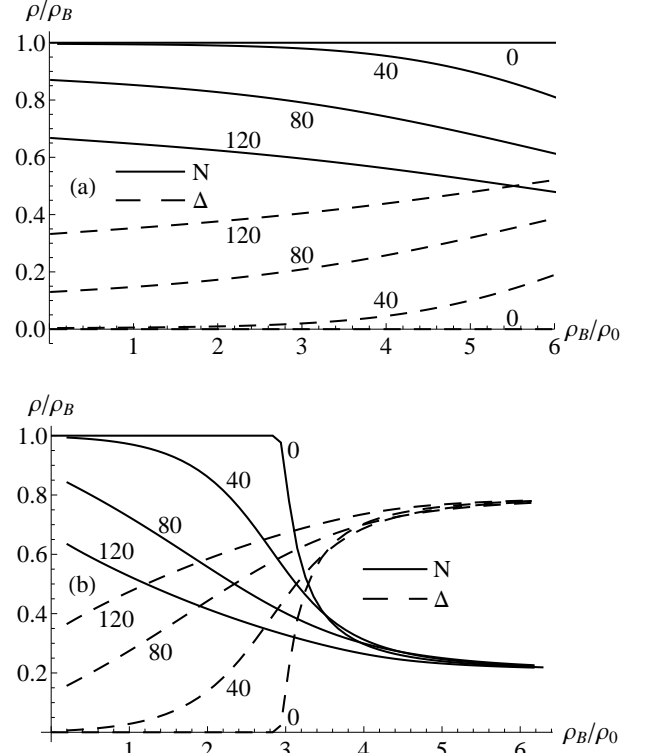
baryon density, different values of particle densities are obtained for different EOSs. To better focus this matter of fact, in Fig. 8, we report the variation of the baryon density, as a function of temperature, for which Δ-isobar density is equal to nucleon density ($\rho_\Delta = \rho_N = \rho_B/2$), for the three different parameters sets. Also in this case, in the comparison, we use comparable values of r_s for different EOSs. As in the previous figure, for the NL$\rho\delta$ parameters set we fix $r_s = 1.32$, corresponding to the value r_s^{II} of Table IV. Analogously, we use $r_s = 1.41$ for GM3 and $r_s = 1.27$ for TM1. As already observed in Fig. 6, for the TM1 parameters set, which has a lower value of M_N^*, the formation of Δ-isobars occurs at lower baryon densities with respect to NL$\rho\delta$ and GM3 (with larger values of M_N^*). Small variations between NL$\rho\delta$ and GM3 correspond mainly to the almost equal saturated nucleon effective mass (slightly greater for the GM3 parameters set).

Finally, in agreement with previous investigations [43, 44], let us observe that, in Fig. 7, the ρ_Δ/ρ_B and ρ_N/ρ_B ratios become constant at sufficiently high baryon density, regardless of the temperature. Increasing the r_s ratio (and fixing r_v) such constant asymptotic values are reached at lower baryon density. Moreover, we have
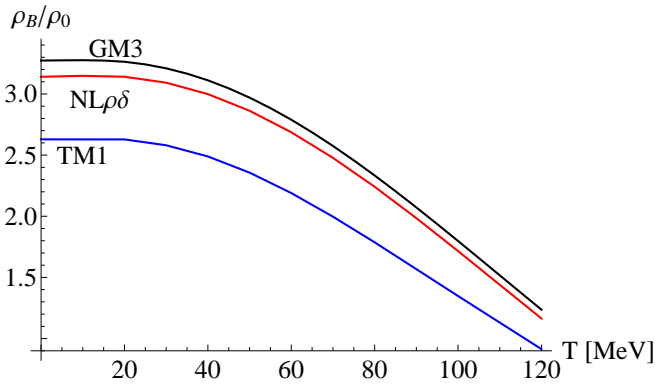
FIG. 8: (Color online) Variation of baryon density, as a function of temperature, for which Δ-isobar density results to be equal to nucleon density, for different parameters sets. The scalar coupling ratios for each EOS are the values $r_s = r_s^{\mathrm{II}}$ reported in Table IV.

verified that this behavior is still realized in asymmetric hadronic matter and even in the presence of hyperons and mesons degrees of freedom. This feature could be an interesting matter of investigation in the future high energy compressed nuclear matter experiments.

B. Equation of state with strange particles

Let us now investigate the EOS with the inclusion of hyperons, non-strange and strange mesons particles at fixed values of Z/A and zero net strangeness, as described in Sec. II.

In Fig. 9, we report the isotherms of the strange chemical potential μ_S (upper panel) and the electric charge chemical potential μ_C (lower panel) for different values of temperature and $Z/A = 0.4$. To point out the role of the Δs degrees of freedom, we have considered three different cases: i) the solid lines do not contain Δ contribution, ii) in the long dashed lines the Δ couplings are $r_s = r_v = 1$, iii) $r_s = 1.3$ and $r_v = 1$ for the short dashed lines. As expected, for a multi-composed strange hadronic matter, μ_S is positive and increases with T and μ_B. At low T we observe very small variations in the strangeness chemical potential with different Δ coupling constants. Very significant effects instead are present in the behavior of μ_C, where, in the presence of the Δ degrees of freedom, we have a sensible reduction of its absolute value and remains almost constant at high μ_B. This matter of fact suppresses the possibility of pion condensation also at very high baryon density (see below for a further discussion on Bose condensation).

Analogously, in Fig.s 10 and 11, we report, for different temperatures and $Z/A = 0.4$, the baryon density and the pressure as a function of the baryon chemical potential. We can see how the presence of the Δ degrees of freedom becomes, already for $T \approx 80$ MeV, very remarkable for baryon densities greater than about $\rho_0/2$. The parame-
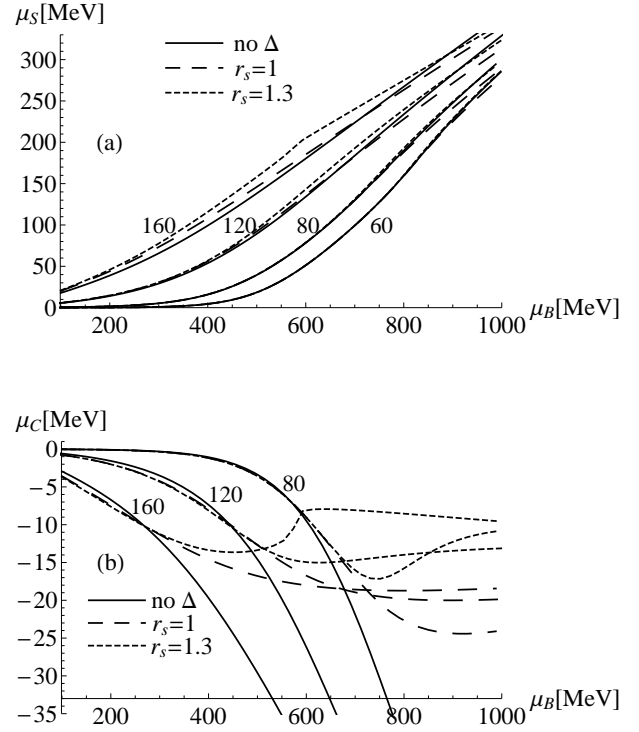

FIG. 9: Variations of the strangeness chemical potential μ_S (upper panel) and electric charge chemical potential μ_C (lower panel) with respect to the baryon chemical μ_B at different values of temperature (in units of MeV) and different Δ coupling constants. The parameters set is GM3 and $r_v = 1$.

ters set used in the above calculations is GM3, however very similar behaviors can be obtained with the other sets. As already remarked, the most relevant difference is that the presence of Δ particles occurs at lower baryon chemical potentials (baryon densities) for the TM1 EOS.

To better understand the relevance of the Δ-isobars, together with the effects of the electric charge fraction and of the effective meson chemical potentials, in Fig. 12, we report the relative difference of the pressure $\Delta P/P$ (without and with Δs contribution) as a function of the baryon chemical potential. The used parameters set is NL$\rho\delta$ but we have common behaviors for all three sets. In the panel (a) and (b) we show the sensibility of the EOS with respect to a variation of Z/A. In fact in the panel (a) $\Delta P(Z/A, \mu^*) \equiv P(Z/A = 0.5) - P(Z/A = 0.4)$ and the symbol μ^* means that we have taken account of effective meson chemical potentials, as described in Sec. II. In the panel (b) is reported the same relative difference but with bare meson chemical potentials μ (in other words, all mesons are considered as a free gas of non-interacting particles). In the figure, the circles, the squares and the triangles represent the values of the baryon chemical potential corresponding to $\rho_B = \rho_0$, $2\rho_0$ and $3\rho_0$, respec-
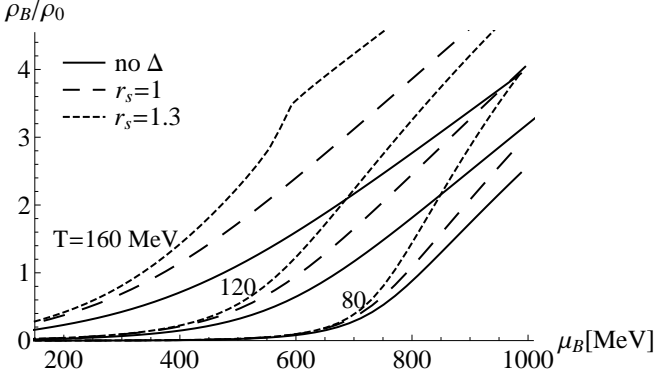
FIG. 10: Baryon density (in units of the nuclear saturation density ρ_0) as a function of the baryon chemical potential μ_B at different values of temperature (in units of MeV). The parameters set is GM3 and $r_v = 1$.
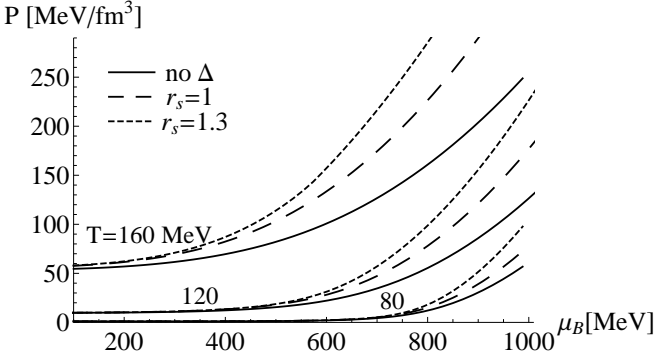

FIG. 11: Pressure as a function of the baryon chemical potential μ_B at different values of temperature (in units of MeV). The parameter set is GM3 and $r_v = 1$.

tively. As expected, the EOS is more sensible to a variation of Z/A at low temperature and this effect decreases by increasing the temperature. However, this behavior is strongly related to the Δ-isobars degrees of freedom. The presence of Δ-isobars greatly reduces the dependence on Z/A in the range of baryon density and temperature relevant in our investigation. This matter of fact is also realized by considering bare meson chemical potentials (panel (b)), even if this effect is less marked. As a consequence, we expect that Δ-isobars degrees of freedom affect significantly the value of the symmetric energy at finite density and temperature.

In the panel (c) and (d) of Fig. 12, we wish to emphasize the importance of effective meson chemical potentials by considering the relative difference between the pressure $P(\mu)$, calculated with bare meson chemical potentials, and the pressure $P(\mu^*)$, including effective meson chemical potentials at fixed ratio $Z/A = 0.4$ (panel (c)) and $Z/A = 0.5$ (panel (d)). The presence of effective meson chemical potentials reflects the behavior of the self-consistent values of the meson fields and, in particular, we

have that its relevance: i) depends on the baryon density (or μ_B), ii) increases with the temperature, iii) depends on the isospin asymmetry (more relevant for asymmetric hadronic matter), iv) decreases with the presence of Δ and the relative difference has a maximum in the region of $\rho_B \approx 0.5 \div 3\rho_0$. We will see in next subsection as these features will be very important in the behavior of the considered particle-antiparticle ratios and in the strangeness production.

Always concerning the role of the effective meson chemical potential, let us further observe that its absolute value is significantly lower than its bare value and, therefore, the window of μ_B and T values, in which Bose condensation can occur, appears to be greatly reduced. Considering, for example, K^+ meson, its bare chemical potential (see Eq.(18)) is $\mu_{K^+} = \mu_S + \mu_C \equiv \mu_p - \mu_\Lambda$, which is dominated from the behavior of μ_S (that increases with μ_B and T, see Fig. 9). However, taking into account Eq.(28), $\mu_{K^+}^*$ is significantly reduced compared to μ_{K^+} by the presence of the ω and ρ mesons fields. At fixed ratio $Z/A = 0.4$ and zero net strangeness, by increasing μ_B and T, the term containing the ρ meson field is always negative but is much smaller than the (positive) ω meson field one and, thus, kaon condensation can occur only at very high baryon densities [73].

C. Particle ratios

We start this subsection by considering, in Fig. 13, the ratio of the net densities Δ^{++}/p as a function of the baryon chemical potential for different values of temperature and different parameters sets. As before, we fix $Z/A = 0.4$. Let us observe that the ratio increases with the temperature but is almost constant with μ_B for $r_s = 1$. On the other hand, it increases rapidly with μ_B if we increase the Δ coupling r_s. In agreement with the previous results of Fig.s 6 and 8, the formation of Δ particles appears to be strongly favored for the TM1 parameters set with respect the other two, especially for $r_s = 1.3$. Let us remember that, in this last case, Δ particles are in different regime depending on the considered parameters sets (see Table IV). The above behavior should be especially evident at low transverse momentum pion spectra in heavy ion collisions at intermediate/high baryon densities and temperatures. Furthermore, remembering that we are not considering decays and rescattering effects, we observe that the order of magnitude of the ratio at high temperature and low density seems to be compatible with the SPS/RHIC experimental results (with measured ratios approximately equal to $0.2 \div 0.5$) [41, 42].

In Fig. 14, we show the variation of K^+/π^+ and K^-/π^- ratios with respect to temperature at various baryon chemical potentials, considering different parameters sets at fixed $r_s = r_v = 1$ coupling ratios. Appreciable variations between the EOSs are observed only at higher baryon chemical potentials ($\mu_B = 600$ MeV). By increasing μ_B we have that the difference between K^+/π^+ and
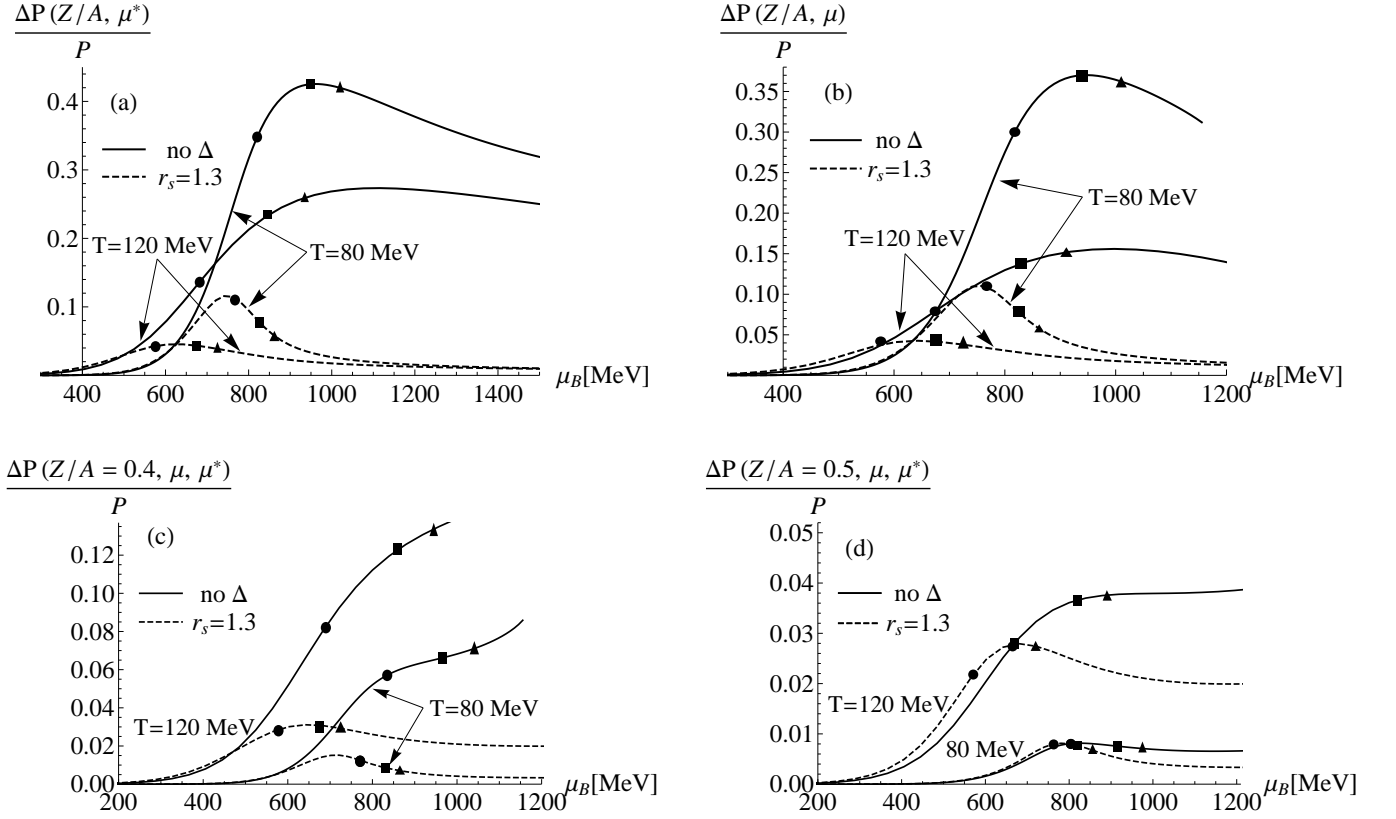
FIG. 12: Relative difference of the pressure as a function of the baryon chemical potential μ_B at different values of temperature with the exclusion (no Δ) and the inclusion ($r_s = 1.3$ and $r_v = 1$) of the Δ-isobars degrees of freedom. Panel (a): $\Delta P(Z/A, \mu^*) \equiv P(Z/A = 0.5) - P(Z/A = 0.4)$ and the symbol μ^* means that we have considered an effective chemical potential for all hadrons (see text for details); panel (b): the same of (a) but mesons have a bare chemical potential (free boson gas); panel (c): $\Delta P(Z/A = 0.4, \mu, \mu^*) \equiv P(\mu) - P(\mu^*)$ at fixed Z/A=0.4, where the pressure $P(\mu)$ is calculated by considering a bare chemical potential for mesons and the pressure $P(\mu^*)$ is calculated by using an effective chemical potential for all hadrons; panel (d): same of (c) but at fixed Z/A=0.5. The circles, the squares and the triangles represent the values of the baryon chemical potential corresponding to $\rho_B = \rho_0$, $2\rho_0$ and $3\rho_0$, respectively.

K^-/π^- ratios increases with the temperature but such a difference becomes much smaller at low μ_B. This behavior is in agreement with recent relativistic heavy ion collisions data [71].

In Fig. 15, we show the ratio K^+/K^- as a function of temperature at different μ_B and Δ coupling ratios (solid lines: absence of Δs, long dashed lines: $r_s = r_v = 1$, short dashed lines: $r_s = 1.3$, $r_v = 1$); $Z/A = 0.4$. As expected, we have a value of the ratio nearly equal to one at low baryon chemical potentials ($\mu_B \leq 300$ MeV), while, for higher μ_B, the ratio has a peak corresponding to baryon density $\rho_B \approx 0.1 \div 0.2\,\rho_0$ for $\mu_B \approx 500 \div 600$ MeV curves. This non-monotonic behavior is much more evident taking into account the Δ-isobars degrees of freedom.

In order to investigate how the previous results depend on the choice of the EOS, in Fig. 16, we report the variation of the K^+/K^- ratio with respect to baryon chemical potential, at fixed temperature $T = 100$ MeV

and for the parameters sets GM3 and TM1 (the results relative to the NL$\rho\delta$ set are not reported because very close to the GM3 ones). As in Fig. 6, we fix the higher value of r_s to the average value r_m between r_s^{II} and r_s^{max} listed in Table IV ($r_m = 1.46$ for GM3 and $r_m = 1.30$ for TM1 parameters set). The two EOSs have similar shapes even if the ratio results to be suppressed at higher μ_B in the TM1 model, also in absence of Δ degrees of freedom. Moreover, a very peculiar behavior appears at $r_s = r_m$ where the ratio has a peak around $\mu_B \approx 640 \div 650$ MeV (corresponding to $\rho_B \approx 0.7\rho_0$ and $\rho_B \approx \rho_0$ for TM1 and GM3 sets, respectively). This feature is mainly due to the fact that, at fixed Z/A and zero net strangeness, the density of K^+ mesons are reduced by the presence of Δ particles.

Related to the above results, it should be interesting to investigate from the experimental point of view the behavior of the ratio K^+/K^- in a kinematical region corresponding to intermediate/high temperatures and high
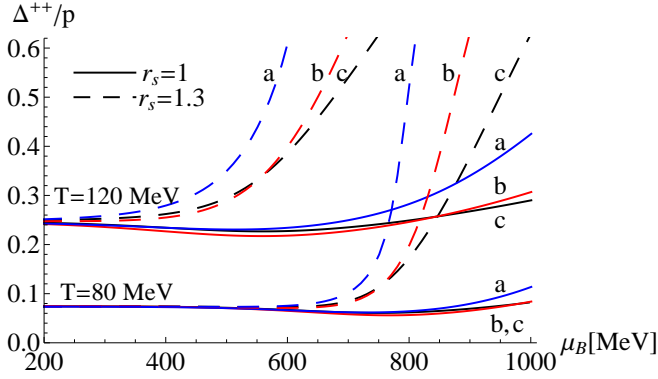
FIG. 13: (Color online) Ratios of net densities Δ^{++}/p as a function of the baryon chemical potential for different temperatures, r_s and parameters sets (a: TM1, b: NL$\rho\delta$, c: GM3).
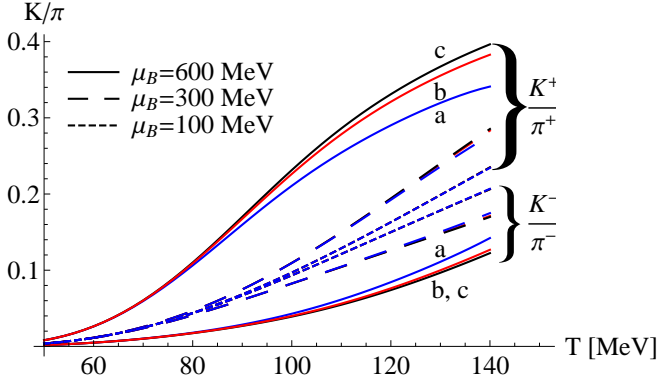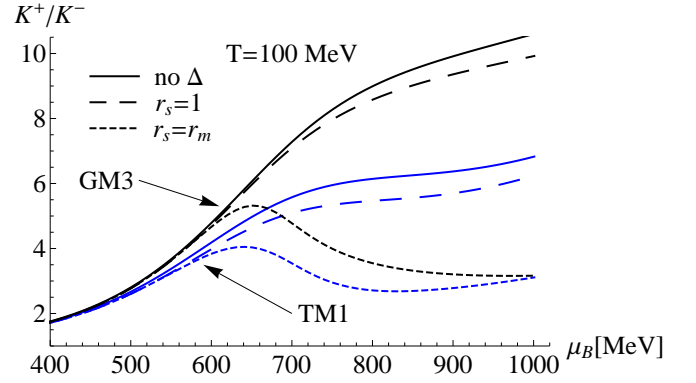

FIG. 16: (Color online) Variation of the K^+/K^- ratio with respect to baryon chemical potential at fixed temperature $T = 100$ MeV. The value r_m corresponds to the average value between r_s^{II} and $r_s^{\max}$ listed in Table IV for the two different parameters sets.

FIG. 14: (Color online) Variation of the K^+/π^+ and K^-/π^- ratios with respect to temperature at different values of baryon chemical potential and different parameters sets (a: TM1, b: NL$\rho\delta$, c: GM3). The Δ coupling ratios are fixed to $r_s = r_v = 1$.
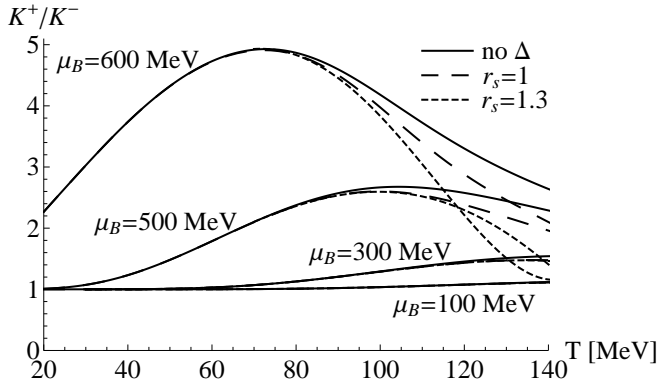
FIG. 15: Variation of the K^+/K^- ratio with respect to temperature at different values of baryon chemical potential and for different Δ coupling ratios (TM1 parameters set).

values of μ_B.

In order to gain a deeper insight about the role of the Δ-isobars and the net electric charge fraction, we report in Figs. 17 and 18 the variation of K^+/π^+ and K^+/K^- ratios with respect to baryon density at $T = 80$ and 120 MeV. For each temperature, we have set: Z/A=0.4 for solid curves and Z/A=0.5 for long dashed curves, both in absence of Δ particles; Z/A=0.4 and Δ couplings $r_s = 1.2$ for short dashed curves; Z/A=0.5 and $r_s = 1.2$ for dotted curves ($r_v = 1$). The parameters set is TM1 but similar behaviors are observed for the other two parameters sets.

Concerning the dependence on Z/A, we have to compare solid with long dashed curves (in absence of Δ particles) and short dashed with dotted ones (with the inclusion of Δs). We can see that the differences between K^+/π^+ ratios are comparable for the two temperatures, while we have a decreasing difference between K^+/K^- ratios by increasing the temperature (it occurs an enhancement of K^+/K^- ratios at $Z/A = 0.5$ with respect to the value $Z/A = 0.4$; the other way round takes place for K^+/π^+ ratios). As already observed in Fig. 12, the presence of the Δ-isobars strongly suppresses the dependence on Z/A for the considered particle ratios. On the other hand, concerning the strangeness production in the presence of the Δ-isobars degrees of freedom, we can compare solid with short dashed curves (at fixed $Z/A = 0.4$) and long dashed curves with the dotted ones (at fixed $Z/A = 0.5$). In agreement with the results of Figs. 14, 15 and 16, we observe that, at fixed T and ρ_B, the presence of the Δ-isobars sensibly decreases both K^+/π^+ and K^+/K^- ratios. Moreover, to outline the importance of the effective meson chemical potential μ^*, in Figs. 17 and 18, we have inserted the dash-dotted curves corresponding to ratios with Z/A=0.4 and Δ coupling $r_s = 1.2$, but with bare meson chemical potentials μ. As already outlined in Fig. 12, comparing these last curves with the

short dashed ones, it is possible to observe the relevance of the effective meson chemical potentials at finite density and temperature and how they thus avoid unphysical too high ratios [71].

Finally, it is interesting to extend the study of the EOS also at high temperatures and low baryon chemical potentials regime. At this scope, in Fig. 19, we report the results of various particle-antiparticle ratios and K^+/π^+ ratio as a function of the $\overline{p}/p$ ratio for different values of temperature. The Δ coupling ratios are fixed to $r_s = r_v = 1$ and $Z/A = 0.4$. The ratios are reported for the GM3 parameters set, however, we have verified that very close results are obtained for the other two parameters sets. Also in this case we can observe good agreements with the results obtained in the framework of statistical-thermal models [18] and with experimental SPS and RHIC data [71].
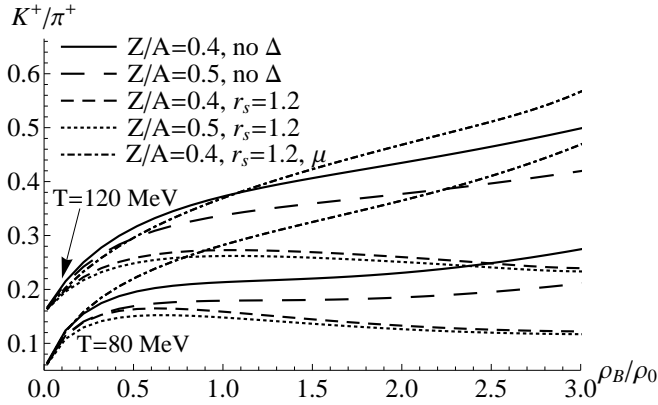

FIG. 17: Variation of K^+/π^+ ratios with respect to baryon density at $T = 80$ MeV (lower curves) and $T = 120$ MeV (upper curves). For the dash-dotted curves the symbol μ indicates that all mesons have bare chemical potentials (see text for details).
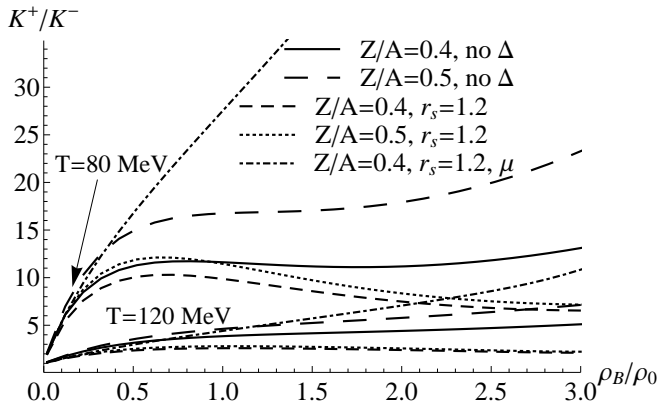

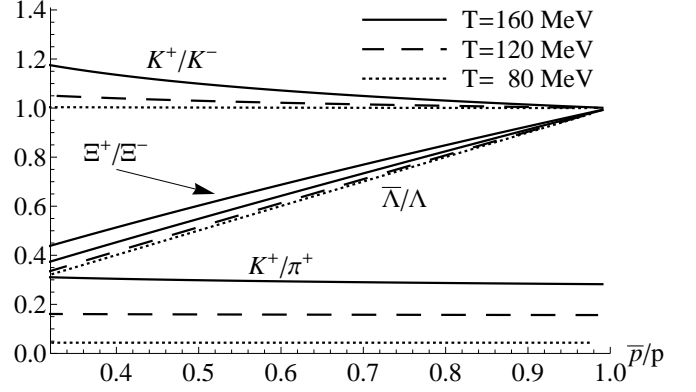FIG. 18: The same of Fig.17 but for K^+/K^- ratios.

FIG. 19: Particle-antiparticle and K^+/π^+ ratios as a function of the $\overline{p}/p$ ratio for different temperatures. The Δ coupling ratios are fixed to $r_s = r_v = 1$. The ratios of Ξ^+/Ξ^- at $T = 80$, 120 MeV are not reported because very strictly to the $\overline{\Lambda}/\Lambda$ ones.

IV. CONCLUSIONS

The main goal of this paper is to show systematically how the presence of the Δ-isobars degrees of freedom affects the hadronic EOS by requiring, in the range of finite density and temperature, the global conservation of baryon number, electric charge fraction and zero net strangeness. In this study we have considered three different parameters sets (GM3, NL$\rho\delta$, TM1) that are compatible with recent analysis at intermediate energy heavy ion collisions and extensively adopted in several applications related to high density β-equilibrium compact stars. We have studied a RMF model with the inclusion of the full octet of baryons and Δ-isobars, self-interacting by means of σ, ρ, ω, δ mesons fields. To take into account the lightest pseudoscalar and vector mesons contribution, especially in regime of low (but finite) baryon density and high temperature, we have incorporated the mesons as an ideal Bose gas but with effective chemical potentials. We have shown that in the EOS and, as a consequence, in the analyzed particle ratios, this assumption appears to be very relevant in the range of density and temperature considered in this paper. The role of the effective meson chemical potential has a phenomenological counterpart in the excluded volume approximation for the hadron resonance gas where all effective particle chemical potentials are shifted, respect to the real ones, proportionally to the particle excluded volume (usually assumed as a parameter). Here, from a more microscopic point of view, the effective meson chemical potentials are shifted proportionally to the mesons fields, related to the self-consistent interaction between baryons.

The relevance of the Δ-isobars in the EOS has been investigated for different parameters sets and coupling ratios at zero and finite temperature, in absence and in presence of hyperons and mesons, for symmetric and

asymmetric nuclear matter. In all considered cases we have shown that the Δ-isobars degrees of freedom play a crucial role. Especially in the range of finite density and temperature considered in the last two subsections, we have seen that: i) the relevance of Δ-isobars strongly increases with a density and temperature increase; ii) at fixed Z/A, the presence of Δ-isobars in the EOS affects significantly the strangeness production; iii) Δ-isobars degrees of freedom remarkably decrease the dependence on the isospin of the EOS and, as a consequence, of the considered particle ratios. This last property appears to be very relevant also in connection to the supposed dependence on Z/A of the critical transition density from hadronic matter to a mixed phase of quarks and hadrons at high baryon and isospin density.

All quoted features are realized even if the Δ-coupling ratios r_s and r_v do not necessarily correspond to the formation of a Δ-isobar metastable state, however, much stronger effects are present if we consider $r_s \gtrsim r_s^{\rm II}$ indicated in Table IV. Furthermore, apart from an appropriate variation of coupling constants, the obtained results are comparable for all three considered parameters sets.

The most relevant difference is that the formation of Δ particles is favored at lower baryon density for the TM1 EOS with respect to the other two parameters sets. This matter of fact is strongly correlated to the significantly lower value of the saturated effective nuclear mass M_N^* in the TM1 parameters set.

Finally, we have investigated several particle-antiparticle ratios and strangeness production as a function of the temperature, baryon density and antiproton to proton ratio. Although the studied EOS is principally devoted to a regime of finite and intermediate values of baryon density and temperature, a satisfactory agreement has been found with recent relativistic heavy ion collisions data and with statistical-thermal models results.

[1] R.C. Hwa and X.N. Wang, *Quark Gluon Plasma 3*, (World Scientific, 2004).
[2] T.S. Biró, J. Phys. G: Nucl. Part. Phys. **35**, 044056 (2008); N. Armesto *et al.*, J. Phys. G: Nucl. Part. Phys. **35**, 054001 (2008).
[3] P. Braun-Munzinger and J. Wambach, Rev. Mod. Phys. **81**, 1031 (2009).
[4] P. Castorina, K. Redlich, H. Satz, Eur. Phys. J. **59**, 67 (2009).
[5] P. Senger, J. Phys. G **30**, S1087 (2004); P. Senger *et al.*, J. Phys. G: Nucl. Part. Phys. **36**, 064037 (2009); W.F. Henning, Nucl. Phys. A **805**, 502 (2008).
[6] I.C. Arsene *et al.*, Phys. Rev. C **75**, 034902 (2007).
[7] L.V. Bravina *et al.*, Phys. Rev. C **78**, 014907 (2008); S. Vogel *et al.*, Phys. Rev. C **78**, 044909 (2008).
[8] S.V. Afanasiev *et al.* (NA49 Collab.), Phys. Rev. C **66**, 054902 (2002).
[9] C. Alt *et al.* (NA49 Collab.), Phys. Rev. C **77**, 024903 (2008).
[10] C. Höhne, Nucl. Phys. A **830**, 369c (2009).
[11] H. Caines (STAR Collab.), arXiv:0906.0305.
[12] T. Sakaguchi (PHENIX Collab.), arXiv:0908.3655.
[13] M. Di Toro *et al.*, Nucl. Phys. A **775**, 102 (2006).
[14] L. Bonanno, A. Drago, and A. Lavagno, Phys. Rev. Lett. **99**, 242301 (2007).
[15] T. Klahn *et al.*, Phys. Rev. C **74**, 035802 (2006).
[16] A. Drago, A. Lavagno, and G. Pagliara, Phys. Rev. D **69**, 057505 (2004); *ibid.*, Phys. Rev. D **71**, 103004 (2005).
[17] P. Braun-Munzinger, J. Stachel, and C. Wetterich, Phys. Lett. B **571**, 36 (2003); A. Andronic, P. Braun-Munzinger, and J. Stachel, Nucl. Phys. A **772** (2006) 167; A. Andronic *et al.*, Nucl. Phys. A **789**, 334 (2007); A. Andronic, P. Braun-Munzinger, and J. Stachel, Phys. Lett. B **673** (2009) 142.
[18] F. Becattini *et al.*, Phys. Rev. C **64**, 024901 (2001); F. Becattini *et al.*, Phys. Rev. C **69**, 024905 (2004); F. Becattini *et al.*, Phys. Rev. C **72**, 064904 (2005); F. Becattini, J. Phys. G: Nucl. Part. Phys. **36**, 064019 (2009).
[19] Z.D. Lu, A. Faessler, C. Fuchs, and E.E. Zabrodin, Phys. Rev. C **66**, 044905 (2002); J. Cleymans, H. Oeschler, K. Redlich, and S. Wheaton, Phys. Rev. C **73**, 034905 (2006); M.I. Gorenstein *et al.*, Phys. Rev. C **79**, 024907 (2009).
[20] R. Hageddorn and J. Rafelski, Phys. Lett. B **97**, 136 (1980).
[21] D.H. Rischke, M.I. Gorenstein, H. Stöcker, and W. Greiner, Z. Phys. C **51**, 485 (1991).
[22] R. Venugopalam and M. Prakash, Nucl. Phys. A **546**, 718 (1992).
[23] G.D. Yen, M.I. Gorenstein, W. Greiner, and S.N. Yang, Phys. Rev. C **56**, 2210 (1997).
[24] M. Mishra and C.P. Singh, Phys. Rev. C **78**, 024910 (2008).
[25] L.M. Satarov, M.N. Dmitriev, and I.N. Mishustin, Phys. of Atomic Nuclei **72**, 1390 (2009).
[26] P. Danielewicz, R. Lacey, and W. G. Lynch, Science **298**, 1592 (2002).
[27] Z. Berezhiani *et al.*, ApJ. **586**, 1250 (2003).
[28] B.D. Serot and J.D. Walecka, Adv. Nucl. Phys. **16**, 1 (1986).
[29] N. K. Glendenning, Phys. Rev. D **46**, 1274 (1992).
[30] J. Theis *et al.*, Phys. Rev. D **28**, 2286 (1983); A. Delfino, M. Jansen, and V.S. Timoteo, Phys. Rev. C **78**, 034909 (2008).
[31] M. Chiapparini *et al.*, Nucl. Phys. A **826**, 178 (2009).
[32] A. Drago, A. Lavagno, and I. Parenti, Ap. J. **659**, 1519 (2007); W.M. Alberico and A. Lavagno, Eur. Phys. J. A **40**, 313 (2009); A. Lavagno and P. Quarati, Phys. Lett. B **498**, 47 (2001).
[33] A.S. Khvorostukhin, V.D. Toneev and D.N. Voskresen-

sky, Nucl. Phys. A **791**, 180 (2007); *ibid.* Nucl. Phys. A **813**, 313 (2008).

[34] D. Zschiesche *et al.*, Phys. Lett. B **547**, 7 (2002).

[35] D. Zschiesche *et al.*, Phys. Rev. C **63**, 025211 (2001); D. Zschiesche *et al.*, J. Phys. G: Nucl. Part. Phys. **31**, 935 (2005); S. Vogel and M. Bleicher, Phys. Rev. C **78**, 064910 (2008).

[36] E. Zabrodin *et al.*, J. Phys. G **36**, 064065 (2009).

[37] M. Hofmann, R. Mattiello, H. Sorge, H. Stöcker, and W. Greiner, Phys. Rev. C **51**, 2095 (1995).

[38] S. Bass, M. Gyulassy, H. Stöcker, and W. Greiner, J. Phys. G: Nucl. Part. Phys. **25**, R1 (1999).

[39] G. Mao, L. Neise, H. Stöcker, and W. Greiner, Phys. Rev. C **59**, 1674 (1999).

[40] J. Schaffner *et al.*, Z. Phys. A **341**, 2414 (1991).

[41] P. Fachini, J. Phys. G: Nucl. Part. Phys. **30**, S735 (2004); **35**, 044032 (2008).

[42] B.I. Abelev *et al.* (STAR Collab.), Phys. Rev. C **78**, 044906 (2008).

[43] B.M. Waldhauser, J. Theis, J.A. Maruhn, H. Stöcker, and W. Greiner, Phys. Rev. C **36**, 1019 (1987).

[44] Z. Li, G. Mao, Y. Zhuo, and W. Greiner, Phys. Rev. C **56**, 1570 (1997).

[45] X. Jin, Phys. Rev. C **51**, 2260 (1995).

[46] D.S. Kosov, C. Fuchs, B.V. Martemyanov, and A. Faessler, Phys. Lett. B **421**, 37 (1998).

[47] Hu Xiang and Guo Hua, Phys. Rev. C **67**, 038801 (2003).

[48] Y. Chen, H. Guo, and Y. Liu, Phys. Rev. C **75**, 035806 (2007); Y. Chen, Y. Yuan, and Y. Liu, Phys. Rev. C **79**, 055802 (2009).

[49] J.D. Walecka, Ann. of Phys. **83**, 491 (1974).

[50] J. Boguta and A.R. Bodmer, Nucl. Phys. A **292**, 413 (1977).

[51] B.D. Serot and J.D. Walecka, Phys. Lett. B **87**, 172 (1979).

[52] B. Liu, V. Greco, V. Baran, M. Colonna, and M. Di Toro, Phys. Rev. C **65**, 045201 (2002).

[53] N.K. Glendenning, Phys. Lett. B **114**, 392 (1982).

[54] A.R. Bodmer, Nucl. Phys. A **526**, 703 (1991).

[55] N.K. Glendenning and S.A. Moszkowski, Phys. Rev. Lett. **67**, 2414 (1991).

[56] G.A. Lalazissis, J. Konig, and P. Ring, Phys. Rev. C **55**, 540 (1997).

[57] Y. Suguhara and H. Toki, Nucl. Phys. A **579**, 557 (1994).

[58] R.J. Furnstahl, J.J. Rusnak and B.D. Serot, Nucl. Phys. A **632**, 607 (1998).

[59] J. Schaffner, C.B. Dover, A. Gal, C. Greiner, and H. Stöcker, Phys. Rev. Lett. **71**, 1328 (1993).

[60] J. Schaffner, C.B. Dover, A. Gal, D.J. Milliner, C. Greiner, and H. Stöcker, Ann. Phys. (N.Y.) **235**, 35 (1994).

[61] R. Knorren, M. Prakash, and P.J. Ellis, Phys. Rev. C **52**, 3470 (1995).

[62] J. Schaffner and I.N. Mishustin, Phys. Rev. C **53**, 1416 (1996).

[63] J.K. Bunta and S. Gmuca, Phys. Rev. C **70**, 054309 (2004).

[64] D.J. Millener, C.B. Dover, and A. Gal, Phys. Rev. C **38**, 2700 (1988).

[65] J. Schaffner-Bielich and A. Gal, Phys. Rev. C **62**, 034311 (2000).

[66] F. Yang and H. Shen, Phys. Rev. C **77**, 025801 (2008).

[67] H. Müller, Nucl. Phys. A **618**, 349 (1997).

[68] H. Müller and B. D. Serot, Phys. Rev. C **52**, 2072 (1995).

[69] G.E. Brown and M. Rho, Nucl. Phys. A **596**, 503 (1996); G.Q. Li, C.-H. Lee, and G.E. Brown, Phys. Rev. Lett. **79**, 5214 (1997).

[70] A. Mishra, S. Schramm, and W. Greiner, Phys. Rev. C **78**, 024901 (2008); S. Banik, W. Greiner, and D. Bandyopadhyay, Phys. Rev. C **78**, 065804 (2008).

[71] B.I. Abelev *et al.* (STAR Collab.), Phys. Rev. C **79**, 034909 (2009) and reference therein.

[72] An analogue assumption, limited to the pions contribution, has been, for example, adopted in Ref.[67].

[73] It is proper to remember that in this approach we are not considering effective meson masses, neglecting, for example, the repulsive potential for kaons and attractive for antikaons [69, 70]. Therefore, differences could occur between the present treatment and more sophisticated formulations. Let us only note here that, in this context, there may be substantial differences between β-equilibrated nuclear matter and hot and dense nuclear matter with zero net strangeness constraint.